J Electr Eng Technol Vol. 9, No. 3: 932-941, 2014
http://dx.doi.org/10.5370/JEET.2014.9.3.932

ISSN(Print) 1975-0102
ISSN(Online) 2093-7423

Autonomous Underwater Vehicles with Modeling and Analysis of 7-Phase BLDC Motor Drives

Sang-Hoon Song*, Yong-Ho Yoon, Byoung-Kuk Lee* and Chung-Yuen Won†**

Abstract – In this paper, a simulation model for 7-phase BLDC motor drives for an Autonomous Underwater Vehicles (AUV) is proposed. A 7-phase BLDC motor is designed and the electrical characteristics are analyzed using FEA program and the power electronics drives for the 7-phase BLDC motor are theoretically analyzed and the actual implementation has been accomplished using Matlab Simulink. PI controller and fuzzy controller are compared for verifying the validity of the proposed model and the informative results are described in detail. Especially A fuzzy controller is used to characterize 7-phase BLDC motor, drive systems under normal and fault operating conditions.

Keywords: AUV, 7-phase BLDC motors, Hysteresis current control, Fuzzy control, PI control.

1. Introduction

The electric motor is equipped into an Autonomous Underwater Vehicle (AUV) as the torpedo propulsion system and it requires high power for short time and high power density with respect of size and weight due to onboard spatial limitation. Among of various types of electric motors, brushless dc (BLDC) motors is regarded as a good candidate for the propulsion system of an AUV due to their high efficiency, high power density, high torque, easy to control, and lower maintenance.

Until now, DC motors have been mainly adopted and tested for this purpose. However, with the requirement of high fault tolerance for military applications, in recent multi-phase BLDC motors have been seriously investigated and, a German newest torpedo adopted 7-phase BLDC motor producing 300kW power [1].

A BLDC motor with higher number of phase has several advantages, compared with the conventional 3-phase one such that it can reduce torque ripple and stator current per phase without increasing voltage and also can increase torque-per-ampere ratio for the same volume, reliability, and power density. In special, for the military application, a motor can be still operated under the malfunction, such as failure condition of one of motor phases, so that it can insure survivability for the system.

Fig. 1 shows the prototype of 7-phase BLDC motor for a small-sized AUV. At the initial stage of development of the 7-phase BLDC motor drive system, one needs a strong simulation program in order to examine the overall electrical and mechanical characteristics of 7-phase BLDC motors for AUV and to test the control algorithms for the drive systems. Specially, the behavior of military machine in health state and under fault condition must be considered in the initial design state of the machine including the each component.

However, one can only refer literatures in the area of 3-phase BLDC motor drives and unfortunately has some trouble to get enough literatures for 7-phase BLDC motor drives [2-4]. Therefore, the aim of this modeling and analysis is to foresee the electrical and mechanical characteristics of 7-phase BLDC motors for AUV and the change of motor performance due to the different faults of the motor drive.

Also different control strategies have been considered for improving the performance of BLDC motors for application in AUV. The PI, the PID controller and the hysteresis current control have been the most widely used control techniques for controlling a BLDC motor. However, the main drawback is the linear nature of classical PID controller that lacks robustness when facing an operation scenario, where parameter variations and disturbances are added to the nominal model [5].

In order to obtain an acceptable dynamic response over the whole operation range, Fuzzy control drive system is attempted in this paper.

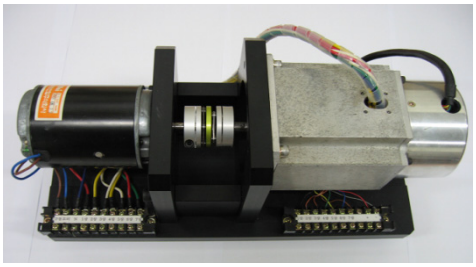

Fig. 1. Prototype of 7-phase BLDC motor for a small-sized AUV

† Corresponding Author: College of Information & Communication Engineering, Sungkyunkwan University, Korea. (woncy@skku.edu)
* College of Information & Communication Engineering, Sungkyunkwan University, Korea. (shsong@ktl.re.kr, bkleeskku@skku.edu)
** New & Renewable Energy Assessment Center, Korea Testing Laboratory (KTL), Korea. (yhyoon@ktl.re.kr)
Received: February 27, 2013; Accepted: January 13, 2014

2. General Description of 7-Phase BLDC Motor Drives

The developed 7-phase BLDC motor has 4 poles and 28 slots. The developed motor has a maximum torque 0.31Nm, maximum speed 10,000rpm, R=0.474Ω, L=0.4mH, and input operating voltage 200Vdc.

The BLDC motor has a permanent-magnet rotor and the stator windings are wounded such that the back electromotive force is trapezoidal. The trapezoidal back EMF implies that the mutual inductance between the stator and rotor is nonsinusoidal. Therefore, no particular advantage exists in transforming the machine equations into the well-known two-axis equations, which is done in the case of machines with sinusoidal back EMF's [6].

The 7-phase currents are controlled to take a type of quasi-square waveform in order to synchronize with the trapezoidal back EMF to produce the constant torque. This task is performed by the speed/torque control loop in cooperation with the rotor position sensor and current controller as shown in Fig. 2.

3. Development of Simulation Model

In this section, the modeling process is explained and the actual implementation using Matlab Simulink is described.

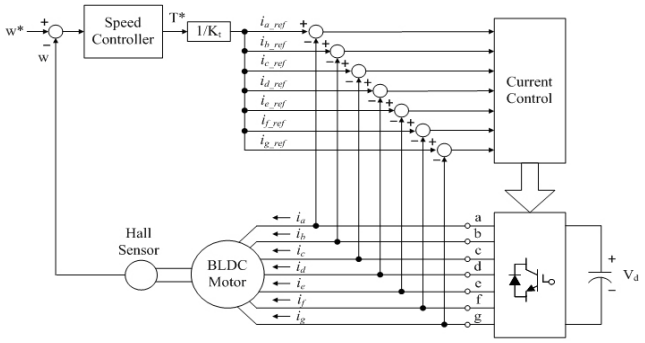

Fig. 2. Control block diagram for 7-phase BLDC motor drives

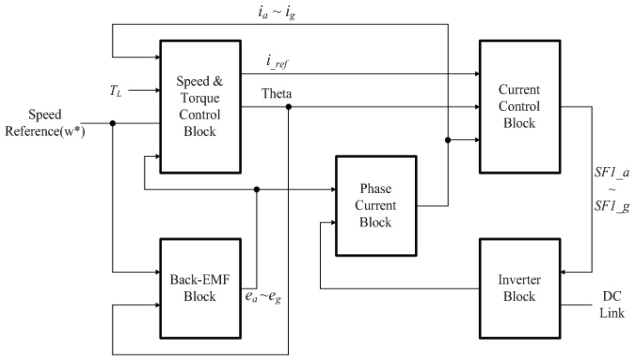

Fig. 3. Overall block diagram of the developed model for 7-phase BLDC motor drives

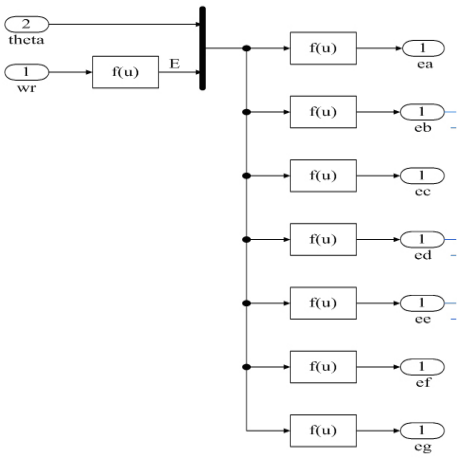

Fig. 4. Implementation of back EMF according to rotor positions

Fig. 3 shows the overall block diagram of the developed model for 7-phase BLDC motor drives. As shown in Fig. 3, the proposed model consists of five functional blocks: back EMF block, phase current block, current control block, PWM inverter block and speed/torque control block [2].

3.1 Back EMF block

The back EMF is a function of rotor position and has the amplitude $E = K_e \cdot \omega_r$ (K_e is the back EMF constant and ω_r is rotor speed). In this paper the modeling of the back EMF is performed under the assumption that all seven phases have identical back EMF waveforms. Based on the rotor position, the numerical expression of back EMF on the case of the phase A can be obtained as Eq. (1) and it is implemented as shown in Fig. 4. Also, the actual back EMF waveform is obtained from the FEA data to examine the actual torque ripple and the detailed information will be explained in "Section 4. Simulation Results."

$$e_a = \begin{cases} (14E/\pi)\theta_r & (0 \le \theta_r < \pi/14) \\ E & (\pi/14 \le \theta_r < 13\pi/14) \\ -(14E/\pi)\theta_r + 14E & (13\pi/14 \le \theta_r < 15\pi/14) \\ -E & (15\pi/14 \le \theta_r < 27\pi/14) \\ (14E/\pi)\theta_r - 28E & (27\pi/14 \le \theta_r < 2\pi) \end{cases} \quad (1)$$

3.2 Phase current and PWM inverter block

The idea is to understand how 7-phase sources are connected under the assumption of floating neutral point. Fig. 5 shows the proposed electrical representation of a 7-phase BLDC motor drive.

The circuit equation of the 7-phase BLDC motor drive including neutral voltage can be represented as

$$[V] = [R] \times [I] + [L_{ij}] \frac{d[I]}{dt} + [E] + [V_{n0}] \quad (2)$$

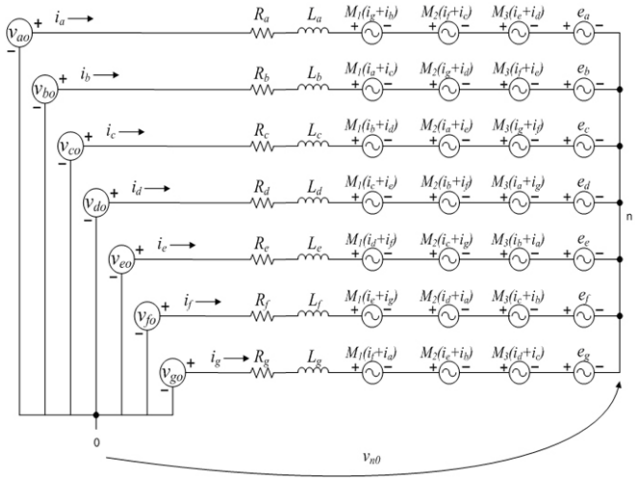

Fig. 5. Electrical representation of 7-phase BLDC motor drives.

where,

phase voltages $[V]=[v_{ao}\ \ v_{bo}\ \ v_{co}\ \ v_{do}\ \ v_{eo}\ \ v_{fo}\ \ v_{go}]^T$,

line resistance $R = R_a = R_b = R_c = R_d = R_e = R_f = R_g$,

winding resistances

$$[R]=\begin{bmatrix} R & 0 & 0 & 0 & 0 & 0 & 0 \\ 0 & R & 0 & 0 & 0 & 0 & 0 \\ 0 & 0 & R & 0 & 0 & 0 & 0 \\ 0 & 0 & 0 & R & 0 & 0 & 0 \\ 0 & 0 & 0 & 0 & R & 0 & 0 \\ 0 & 0 & 0 & 0 & 0 & R & 0 \\ 0 & 0 & 0 & 0 & 0 & 0 & R \end{bmatrix}$$

phase currents $[I]=[i_a\ \ i_b\ \ i_c\ \ i_d\ \ i_e\ \ i_f\ \ i_g]^T$,

inductance of phase *i* related to phase *j*

$$[L_{ij}]=\begin{bmatrix} L_a & M_{ab} & M_{ac} & M_{ad} & M_{ae} & M_{af} & M_{ag} \\ M_{ba} & L_b & M_{bc} & M_{bd} & M_{be} & M_{bf} & M_{bg} \\ M_{ca} & M_{cb} & L_c & M_{cd} & M_{ce} & M_{cf} & M_{cg} \\ M_{da} & M_{db} & M_{dc} & L_d & M_{de} & M_{df} & M_{dg} \\ M_{ea} & M_{eb} & M_{ec} & M_{ed} & L_e & M_{eg} & M_{eg} \\ M_{fa} & M_{fb} & M_{fc} & M_{fd} & M_{fe} & L_f & M_{fg} \\ M_{ga} & M_{gb} & M_{gc} & M_{gd} & M_{ge} & M_{gf} & L_g \end{bmatrix}$$

back EMF $[E]=[e_a\ \ e_b\ \ e_c\ \ e_d\ \ e_e\ \ e_f\ \ e_g]^T$,

neutral voltages $[V_{no}]=[v_{no}\ v_{no}\ v_{no}\ v_{no}\ v_{no}\ v_{no}\ v_{no}]^T$.

For a balanced wye-connected BLDC motor, the 7-phase currents always meet the following equation:

$$i_a + i_b + i_c + i_d + i_e + i_f + i_g = 0 \tag{3}$$

Therefore, the neutral voltage v_{no} can be simplified as

$$v_{no} = \frac{1}{7}\sum_{i=a}^{g} v_{io} \tag{4}$$

Substituting (4) into (2) gives

$$[K]\times[V] = [R]\times[I] + [L_{ij}]\frac{d[I]}{dt} + [E] \tag{5}$$

where,

$$[K]=\frac{1}{7}\begin{bmatrix} 6 & -1 & -1 & -1 & -1 & -1 & -1 \\ -1 & 6 & -1 & -1 & -1 & -1 & -1 \\ -1 & -1 & 6 & -1 & -1 & -1 & -1 \\ -1 & -1 & -1 & 6 & -1 & -1 & -1 \\ -1 & -1 & -1 & -1 & 6 & -1 & -1 \\ -1 & -1 & -1 & -1 & -1 & 6 & -1 \\ -1 & -1 & -1 & -1 & -1 & -1 & 6 \end{bmatrix}$$

Each self-inductance and mutual inductance can be defined as follows:

$$L_{aa} = L_{bb} = L_{cc} = L_{dd} = L_{ee} = L_{ff} = L_{gg} = L_s \tag{6}$$

$$\begin{aligned} M_{ag} &= M_{ab} = M_{ba} = M_{bc} = M_{cb} = M_{cd} = M_{dc} = M_{de} \\ &= M_{ed} = M_{ef} = M_{fe} = M_{fg} = M_{gf} = M_{ga} = M_1 \end{aligned} \tag{7}$$

$$\begin{aligned} M_{af} &= M_{ac} = M_{bg} = M_{bd} = M_{ca} = M_{ce} = M_{db} = M_{df} \\ &= M_{ec} = M_{eg} = M_{fd} = M_{fa} = M_{ge} = M_{gb} = M_2 \end{aligned} \tag{8}$$

$$\begin{aligned} M_{ae} &= M_{ad} = M_{bf} = M_{be} = M_{cg} = M_{cf} = M_{da} = M_{dg} \\ &= M_{eb} = M_{ea} = M_{fc} = M_{fb} = M_{gd} = M_{gc} = M_3 \end{aligned} \tag{9}$$

Therefore, Eq. (5) can be rewritten as Eq. (10).

$$[L_{eq}]\frac{d[I]}{dt} = [K]\times[V] - [R]\times[I] - [E] \tag{10}$$

where,

$$[L_{eq}]=\begin{bmatrix} L_s & M_1 & M_2 & M_3 & M_3 & M_2 & M_1 \\ M_1 & L_s & M_1 & M_2 & M_3 & M_3 & M_2 \\ M_2 & M_1 & L_s & M_1 & M_2 & M_3 & M_3 \\ M_3 & M_2 & M_1 & L_s & M_1 & M_2 & M_3 \\ M_3 & M_3 & M_2 & M_1 & L_s & M_1 & M_2 \\ M_2 & M_3 & M_3 & M_2 & M_1 & L_s & M_1 \\ M_1 & M_2 & M_3 & M_3 & M_2 & M_1 & L_s \end{bmatrix}$$

Each phase voltages can be derived as Eq. (11) using

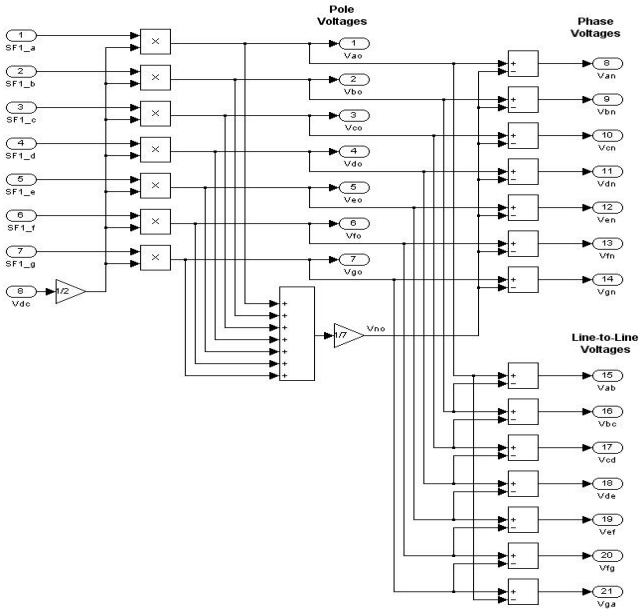

Fig. 6. Implementation of phase voltages

switching function $SF_{1\_a,b,c,d,e,f,g}$ obtained from current control block. Based on the derived switching function, one can generate pole voltages (V_{ao}, V_{bo}, V_{co}, V_{do}, V_{eo}, V_{fo}, V_{go}) by multiplying the half of dc-link voltage and phase voltages and line-to-line voltage can be easily obtained as following equations. The voltage generation process can be expressed as Eqs. (11) and (12) and it can be implemented as shown in Fig. 6.

$$\begin{bmatrix} v_{ao} = \frac{V_d}{2} SF_{1\_a}, v_{bo} = \frac{V_d}{2} SF_{1\_b}, v_{co} = \frac{V_d}{2} SF_{1\_c} \\ v_{do} = \frac{V_d}{2} SF_{1\_d}, v_{eo} = \frac{V_d}{2} SF_{1\_e}, v_{fo} = \frac{V_d}{2} SF_{1\_f} \\ v_{go} = \frac{V_d}{2} SF_{1\_g} \end{bmatrix} \tag{11}$$

$$\begin{bmatrix} v_{ab} = v_{ao} - v_{bo}, v_{bc} = v_{bo} - v_{co}, v_{cd} = v_{co} - v_{do}, v_{de} = v_{do} - v_{eo} \\ v_{ef} = v_{eo} - v_{fo}, v_{fg} = v_{fo} - v_{go}, v_{ga} = v_{go} - v_{ao} \\ v_{no} = \frac{1}{7}\left(v_{ao} + v_{bo} + v_{co} + v_{do} + v_{eo} + v_{fo} + v_{go}\right) \\ v_{an} = v_{ao} - v_{no}, v_{bn} = v_{bo} - v_{no}, v_{cn} = v_{co} - v_{no}, v_{dn} = v_{do} - v_{no} \\ v_{en} = v_{eo} - v_{no}, v_{fn} = v_{fo} - v_{no}, v_{gn} = v_{go} - v_{no} \end{bmatrix} \tag{12}$$

As noted from Eqs. (11) and (12), it is important to select the proper pattern for switching functions for the entire simulation program according to the pwm algorithms. In case of Sinusoidal PWM (SPWM), the switching functions can be obtained by comparing triangular and sinusoidal control signals. In case of BLDC motor drives, the switching functions can be obtained from hysteresis current control algorithm, which will be explained in the next Section.

3.3 Current control block

The current control strategies of the BLDC motor drive are typically grouped into pulse with modulation technique and hysteresis technique. In this paper, bipolar hysteresis current control is used for obtaining the fast dynamic response during the transient states.

In order to express the exact phenomena of current dynamics, the phase current needs to be modeled into four modes as show in Fig. 7, such as $I_a < lower\lim it(LL)$ (mode [1]), $I_a > upper\lim it(UL)$ (mode [2]), $LL < I_a < UL$ and $\frac{dI_a}{dt} > 0$ (mode [3]), and $LL < I_a < UL$ and $\frac{dI_a}{dt} < 0$ (mode [4]).

$$\begin{aligned} f_a(u) = {} & (u[4] \ge \pi/14) \times (u[4] < 13\pi/14) \times \\ & \begin{bmatrix} (u[1] < u[3] \times 0.95) - (u[1] > u[3] \times 1.05) \\ +(u[1] > u[3] \times 0.95) \times (u[1] < u[3] \times 1.05) \times (u[1] > u[2]) \\ -(u[1] > u[3] \times 0.95) \times (u[1] < u[3] \times 1.05) \times (u[1] < u[2]) \end{bmatrix} \\ & +(u[4] \ge 15\pi/14) \times (u[4] < 27\pi/14) \times \\ & \begin{bmatrix} -(u[1] > -u[3] \times 0.95) + (u[1] < -u[3] \times 1.05) \\ -(u[1] < -u[3] \times 0.95) \times (u[1] > -u[3] \times 1.05) \times (u[1] < u[2]) \\ +(u[1] < -u[3] \times 0.95) \times (u[1] > -u[3] \times 1.05) \times (u[1] > u[2]) \end{bmatrix} \end{aligned} \tag{13}$$

In Matlab Simulink, in order to express modes [3] and [4], the memory block is used along with rotor position (Θ_r) as shown in Fig. 8 and finally the entire current dynamics can be realized using Eq. (13).

In this model the switching function SF_1 is used to generate the inverter phase voltages. Therefore, each phase current can be obtained by

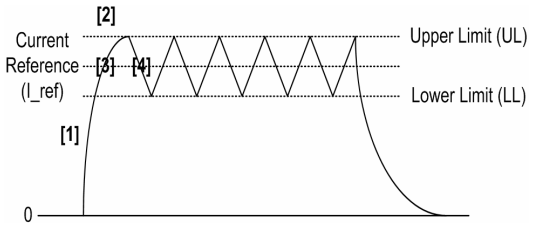

Fig. 7. Detailed current modes to model its dynamics

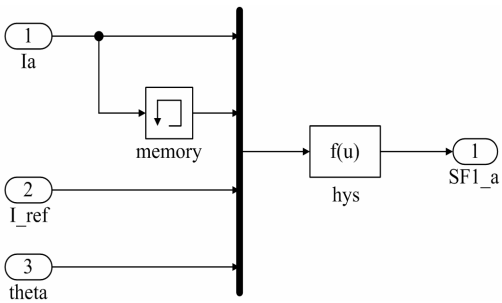

Fig. 8. Hysteresis current control block for phase A

$$[L_{eq}]\frac{d[I]}{dt}=[K]\times\frac{V_d}{2}[SF_1]-[R]\times[I]-[E] \quad (14)$$

where,

$$[SF_1]=[SF_{1\_a}\ \ SF_{1\_b}\ \ SF_{1\_c}\ \ SF_{1\_d}\ \ SF_{1\_e}\ \ SF_{1\_f}\ \ SF_{1\_g}]^T$$

3.4 Speed/Torque control block

The electromagnetic torque is expressed as

$$T_e=\frac{\sum_{i=a}^{g}(e_i\times i_i)}{\omega_r} \quad (15)$$

And the equation of motion is expressed as

$$\frac{d}{dt}\omega_r=(T_e-T_L-B\omega_r)/J \quad (16)$$

where, T_L is load torque, J is inertia, and B is damping.

Neglecting the damping factor, speed and torque characteristics of the BLDC motor can be explained as

$$\omega_r=\frac{1}{J}\int(T_e-T_L)dt \quad (17)$$

Using PI controller, the speed and torque control can be implemented as shown in Fig. 9.

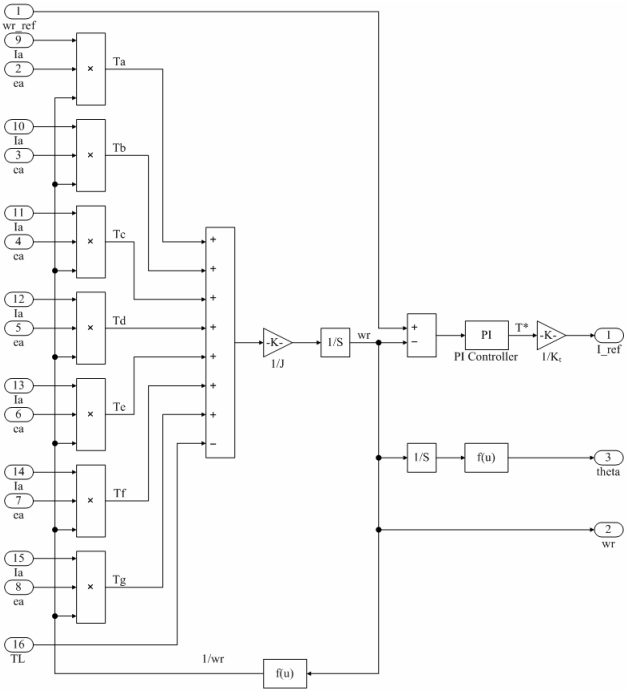

Fig. 9. Speed and torque control block for 7-phase BLDC motor drives

4. Simulation Result

A 7-phase BLDC motor drive with proposed model has been simulated with the following specifications: 7-phase, 4 poles, rated torque of 0.15Nm, rated speed of 10,000 rpm, V_{dc}=200V, R=0.474Ω, L=394uH, K_t=0.2226, J = 0.00132 kgm^2, M_1 = 21.87uH, M_2 = 130uH, M_3 = 78.73uH.

Fig. 10 shows the back EMF computed according to the previously discussed procedure using Eq. (1) at 3,500 rpm. The rotor position is varied from 0 to 2π per electric cycle 2π /7 and the back EMF has amplitude of 19.5V.

Figs. 11 and 12 show the generated phase current, dynamic responses of speed and current command waveforms by the PI controller at 3,500 rpm. The phase current has amplitude of 1.8A and is well synchronized with the trapezoidal back EMF. Also to demonstrate the speed dynamic response of the PI controller algorithm, the speed response characteristic is shown in Fig. 2 along with the reference speed change.

Figs. 13 and 14 show the generated phase current,

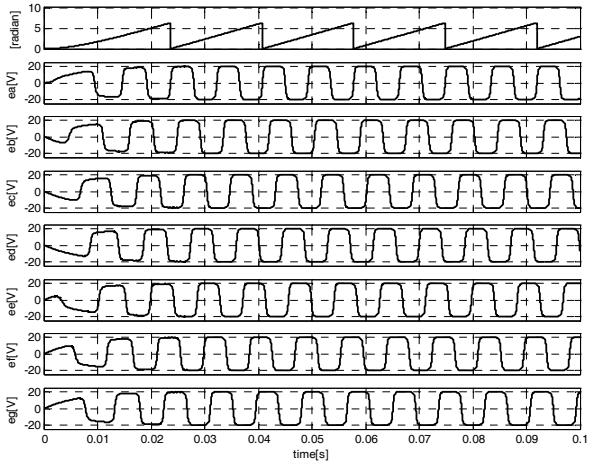

Fig. 10. Back EMF waveforms at 3,500 rpm

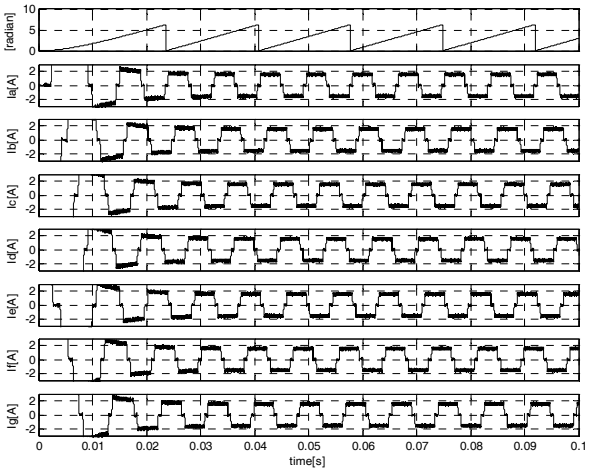

Fig. 11. Phase current waveforms by a PI controller (3,500 [rpm]).

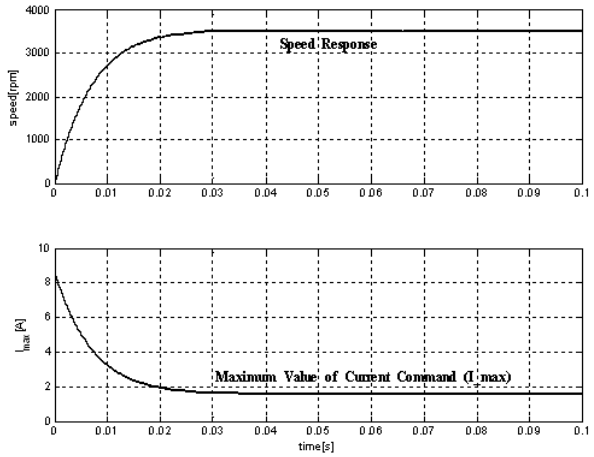

Fig. 12. Speed response and current command by the PI controller (3,500[rpm]).

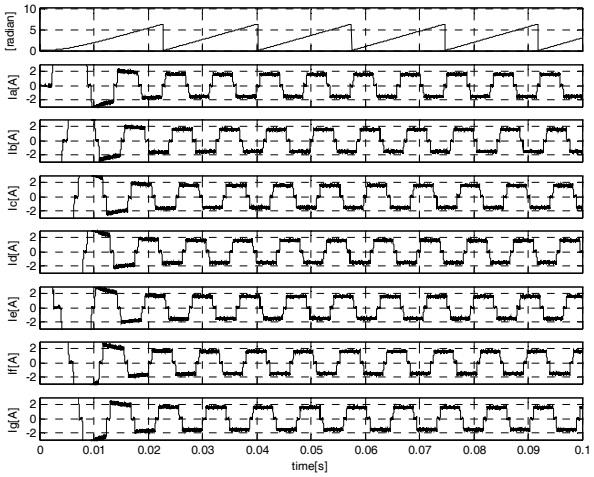

Fig. 13. Phase current waveforms by a Fuzzy controller (3,500[rpm]).

dynamic responses of speed and current command waveforms by the fuzzy controller at 3,500 rpm. The phase current has amplitude of 1.8A and is well synchronized with the trapezoidal back EMF. Also to demonstrate the speed dynamic response of the Fuzzy controller algorithm, the speed response characteristic is shown in Fig.14 along with the reference speed change. In comparison with PI controller, the speed response characteristic of Fuzzy controller is shown the no difference.

In order to examine the feasibility on phase fault tolerance characteristics of the developed simulation program, one of phase is forcibly shorted, phases A and B phase are opened at the same time and the overall characteristics are examined and the results of overall characteristics are examined as shown Fig. 15 and Fig. 16.

After the fault occurrence one notice the increase of the average value of the healthy phase-current, due to the reaction of the superimposed speed loop; the appearance of fluctuations in the rotor speed depends to the incoming torque ripple. Nevertheless the operation is maintained at

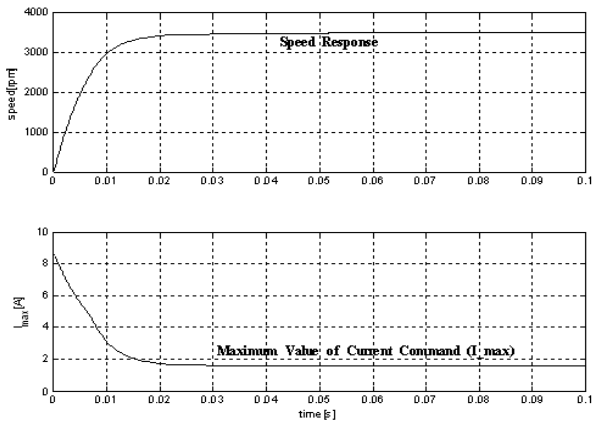

Fig. 14. Speed response and current command by the Fuzzy controller (3,500[rpm]).

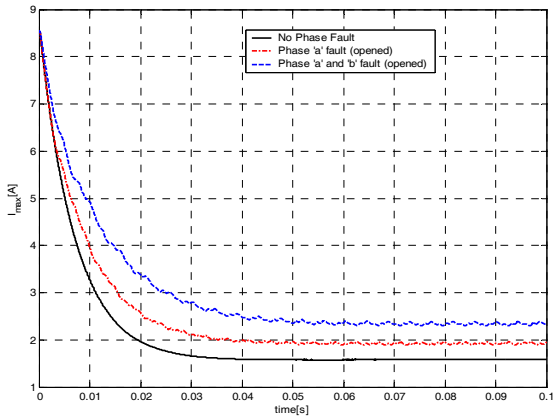

Fig. 15. Current command waveforms at 3,500[rpm] in case of phase fault (opened) conditions.

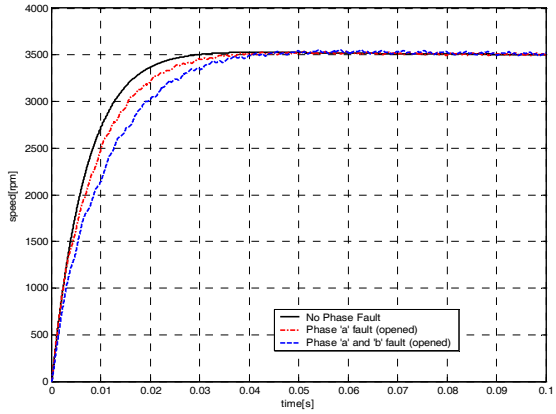

Fig. 16. Speed response waveforms at 3,500[rpm] in case of phase fault (opened) conditions.

preset speed and load conditions.

Comparing with the fault condition, as one can expect, the fault condition of phases A and B makes the drive system be deteriorated with respect of speed response in special.

From the simulation results of Figs. 15 to 16, it is

certified that the developed simulation program can effectively examine the dynamic characteristics at fault condition as well as at healthy condition of 7-phase BLDC motor drives for AUV.

5. Experimental Result

A schematic diagram of the proposed drive system of 7-phase BLDC motor, which corresponds to the experimental system is designed, developed and presented in Fig. 15.

The experimental setup consists of four major components.

They are IGBT power inverter, 7-phase BLDC motor with loading arrangement, speed, phase voltage and phase current sensing circuits, and TMS320VC33-150 DSP. The BLDC motor is an electronically commutated motor.

The built-in hall sensors generate seven signals according to the rotor position. These signals are decoded to identify the rotor position and energize the appropriate windings by switching the appropriate switches in the IGBT power inverter. Experimental results of 7-phase BLDC motor speed control with Fuzzy control will be compared with the results of BLDC motor speed control only with PI control.

The experimental results obtained for Fuzzy controller-based BLDC motor drive under different operating conditions such as step change in reference speed, and with load disturbance are shown in Fig. 19, Figs. 21 and Fig. 23 in comparison with PI controller.

Figs. 18-19 show the phase current waveforms when the 7-phase motor operated at the steady state mode by each controller (Fuzzy, PI) respectively.

In another test, step changing has exerted in motor command speed as shown in Figs. 20~21. Speed command changing has been in case: increasing speed command 3500, 7,000, 10,000rpm respectively with speed controller. In step increasing speed, first motor command speed is 3,500rpm. Reference speed is changed to 7,000 rpm and another increasing speed, primary motor speed is 10,000 rpm which is increased to 10,000 rpm. Rising time in each case(PI controller, Fuzzy controller) is nearly 2.5~3sec. But there are some overshoot and steady state error in responses at the sudden change speed mode with PI controller. Also we know that there is no overshoot in response at 10,000rpm with Fuzzy controller and steady state error is dispensable as shown in Fig. 21. Therefore we

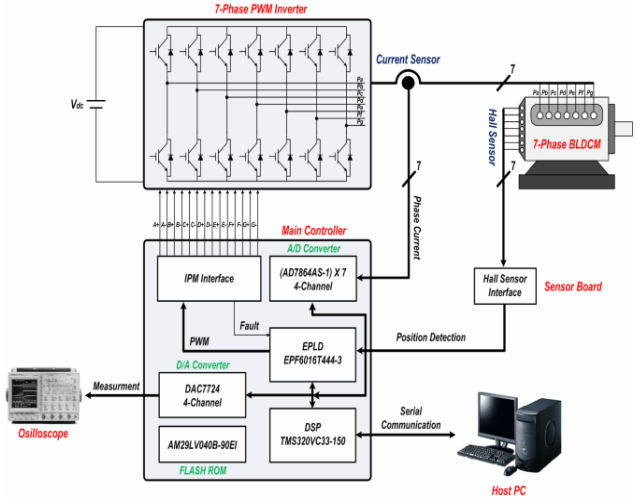

Fig. 17. Block diagram of experimental system.

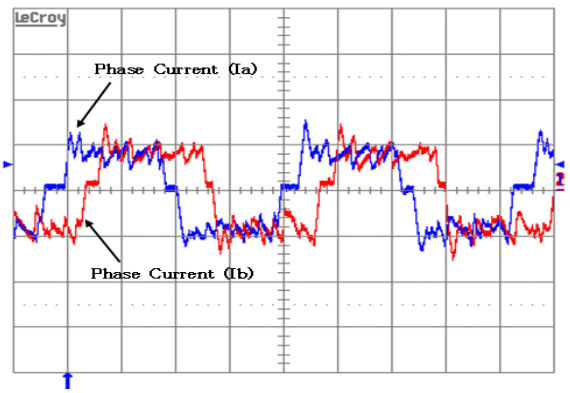

Fig. 18. Current waveforms of phase A and B by the PI controller. (2ms, 2A/div., 3,500rpm)

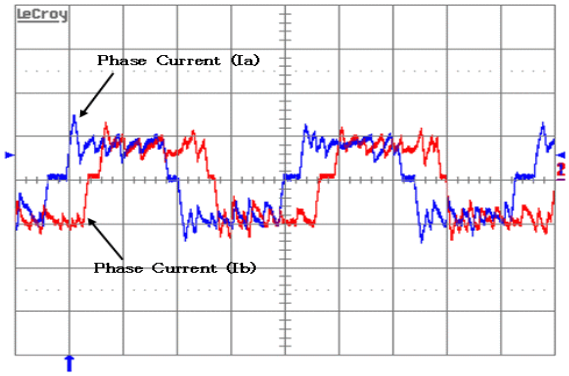

Fig. 19. Current waveforms of phase A and B by the Fuzzy controller. (2ms, 2A/div., 3,500rpm)

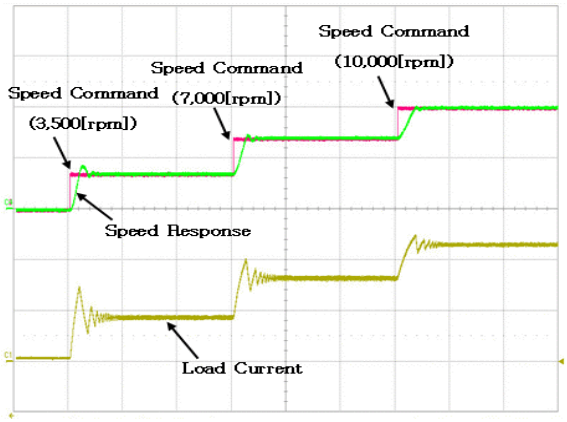

Fig. 20. Speed response by the PI controller with load at three-step speed. (5s, 1A/div.)

have achieved the high speed control of BLDC motor to yield excellent performance with Fuzzy controller.

Also to demonstrate the speed dynamic response with no load, speed response waveforms at increasing and decreasing speed reference by each controller (Fuzzy, PI) respectively as shown in Figs. 22-23. When speed reference 0→2,500→5,000rpm changed, 7-phase BLDC motor operated at the steady state mode by each controller (Fuzzy, PI).

But in case of using PI controller, it is found that speed response characteristics are unstable in comparison Fuzzy controller at the 2500rpm mode, 5,000rpm mode. On the other hand when speed reference 5,000→ 2,500→0rpm changed, it is noted that speed response characteristics of 7-phase BLDC motor by each controller (Fuzzy, PI) are same results.

The variation of load current and speed response due to change in load applied to the 7-phase BLDC motor is shown in Fig. 24-27. Firstly to examine the performance of the 7-phase BLDC motor with each controller algorithm, it is loaded, the rated torque demand in this case is 0.2Nm and the motor speed is 15,000 rpm at the Fig. 24~25. It is certified that Fuzzy controller algorithm is successfully controlled with a small speed ripple compared with PI controller when load applied and speed changed

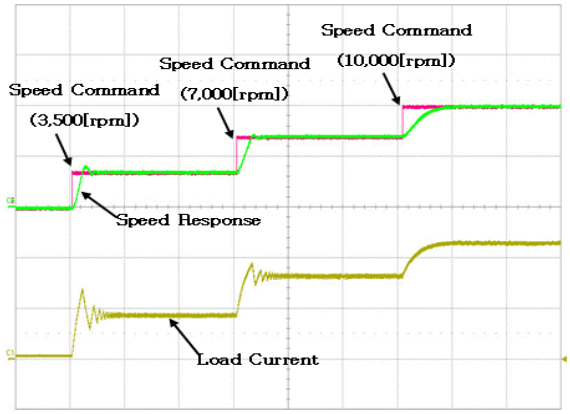

Fig. 21. Speed response by the Fuzzy controller with load at three-step speeds. (5s, 1A/div.)

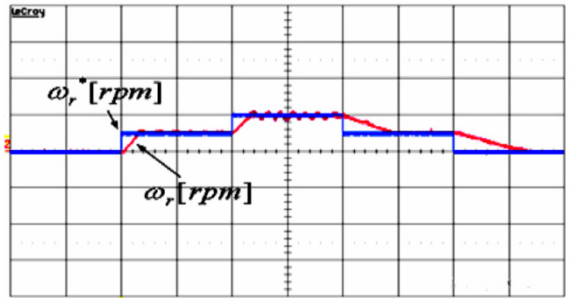

Fig. 22. Speed response by the PI controller with no load at increasing and decreasing speeds. (5s/div., 0 → 2,500→5,000→2,500→0 rpm)

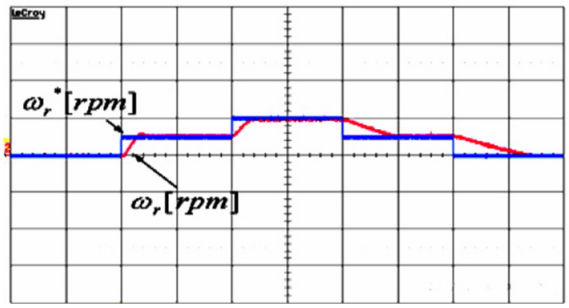

Fig. 23. Speed response by the Fuzzy controller with no load at increasing and decreasing speeds. (5s/div., 0→2,500→5,000→2,500→0 rpm)

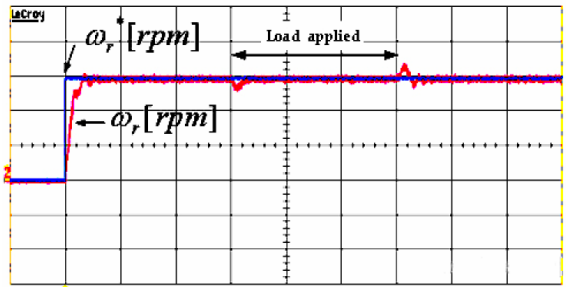

Fig. 24. Speed response and load application test of the PI controller (10s/div., 15,000rpm, 0.2Nm)

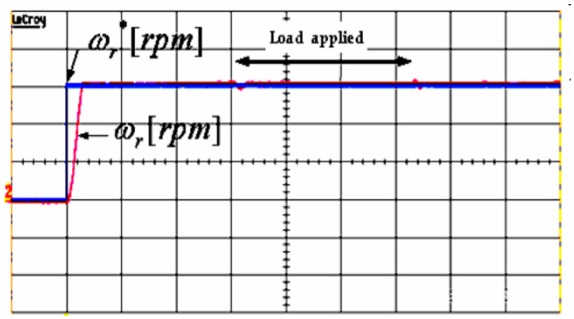

Fig. 25. Speed response and load application test of the Fuzzy controller (10s/div., 15,000rpm, 0.2Nm)

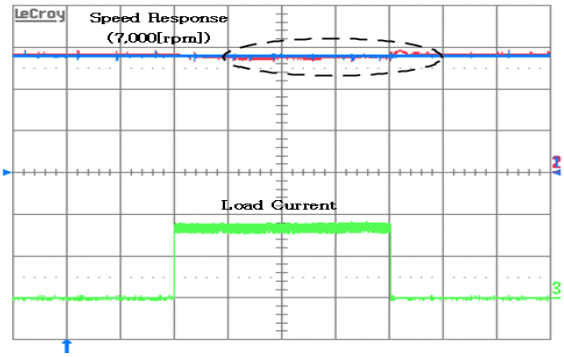

Fig. 26. Load application test of the PI controller (1s, 1V, 2A/div., 7,000rpm, 0.1Nm)

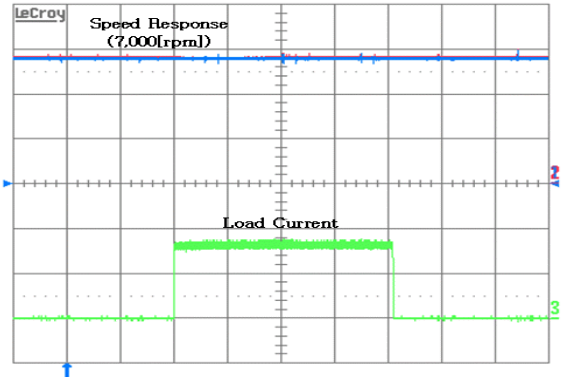

Fig. 27. Load application test of the Fuzzy controller. (1s, 1V, 2A/div., 7,000rpm, 0.1Nm)

Next, the torque developed by the 7-phase BLDC motor at 7,000rpm is 0.1Nm load applied to 7-phase BLDC motor at the Fig. 26~27. It is found that speed response of PI controller is unstable when there is a sudden increase in load. But speed response of Fuzzy controller is very stable when increase in load.

The experimental results clearly show that Fuzzy controller based 7-phase BLDC motor drive can provide an improved speed response with consistently when the system is subjected to load disturbance and step change in reference speed.

5. Conclusion

The propulsion motor for the autonomous underwater vehicle requires high torque, small size, and fault tolerance. Consequently, a multiphase permanent magnet brushless motor fits AUV electric propulsions.

In this paper, a functional simulation model for the 7-phase BLDC motor drive is studied and the actual implementation of the model is proposed. The performance and feasibilities have been examined by the simulation and experimental verification and it is expected that the proposed simulation model can be utilized for the development of AUV systems. Also since the fuzzy control system is easy to design and implement, effective in dealing with the uncertainties and parameter variations, and has better overall performance, fuzzy controller-based 7-phase BLDC motor drive system may be preferred over PI controller-based 7-phase BLDC motor drive for automation, robotics, position and velocity control systems, and industrial control applications.

References

[1] C. V. Alt. Autonomous underwater vehicles. Autonomous Underwater Lagrangian Platforms and Sensors Workshop, 2003. p.1-5.

[2] B. K. Lee and M. Ehsani. Advanced simulation model for brushless dc motor drives. Electric Power Components and Systems 2003. P. 841-868.

[3] S. K. Safi, P. P. Acarnley, and A. G. Jack. Analysis and simulation of the high-speed torque performance of brushless dc motor drives. In: Proceeding of the IEE, 1995. p.191-200.

[4] N. N. Franceschetti and M. G. Simoes. A new approach for analysis, modeling, and simulation of brushless multiphase machines. In: Proceeding of IEEE-ICON. 2001. p.1423-1427.

[5] M. Dias, J. P. da Costa, H. Einfeld, P. Zacharias. High Performance Controller for Multiphase Brushless DC Motor. In: Proceeding of ICEM. 2012. p.967-972.

[6] P. Pillay and R. Krishnan. Modeling, simulation, and analysis of permanent-magnet motor drives Part II: The brushless dc motor drive. IEEE Trans. on Industry Applications 1989. p. 274-279.

[7] Ion Boldea, Lucian-Nicolae Tutelea, Dragos Ursu. BLDC Multiphase Reluctance Machines for Wide Range Applications: a revival attempt. In: Proceeding of EPE-PEMC. 2012.

[8] Claudiu Oprea, Claudia Martis, Biro Karoly. Six-phase Brushless DC Motor for Fault Tolerant Electric Power Steering Systems. In: Proceeding of ACEMP. 2007.

[9] Tae-Hyung Kim, Hyung-Woo Lee, Mehrdad Ehsani. Advanced Sensorless Drive Technique for Multiphase BLDC Motors. In: Proceeding of IES. 2004. p. 926-931

[10] Hao Xiong, Qiang Wu, Yuqi Rang, Guangwei Meng, Huaishu Li, Libing Zhou. Analysis and Simulation of High Power Multi-Phase BLDC Motor. In: Proceeding of AIMSEC. 2011. p. 3751-3754.

Sang-Hoon Song was born in Korea, in 1972. He received the B.S degree in Electrical Engineering from the Yeungnam Univ. in1998, and the M.S from the Sungkyunkwan Univ. Korea, in 2000. He currently studies for his Ph. D degree in Sungkyunkwan Univ. and has researched for the Korea Testing Laboratory from 2000.

Yong-Ho Yoon received the M.S. and Ph.D. degrees in Mechatronics Engineering from Sungkyunkwan University, Korea, in 2002, 2007, respectively. From 2007 to 2011, he was with Technical Research Institute of Samsung Thales Company, Korea, as a senior researcher. Since 2011, he has been with

Korea Testing Laboratory (KTL), where he is currently a senior researcher in the New & Renewable Energy Assessment Center, Machinery & System Division. His research interests are in the areas of analysis and control of SRM and BLDC motor and certification of renewable of photovoltaic Inverter.

Byoung-Kuk Lee (S'97-M'02-SM'04) received the B.S. and M.S. degrees from Hanyang University, Seoul, Korea, in 1994 and 1996, respectively, and the Ph.D. degree from Texas A&M University, College Station, TX, USA, in 2001, all in electrical engineering. From 2003 to 2005, he was a Senior Researcher at Power Electronics Group, Korea Electrotechnology Research Institute, Changwon, Korea. He joined the School of Information and Communication Engineering, Sungkyunkwan University, Suwon, Korea, in 2006. His research interests include charger for electric vehicles, hybrid renewable energy systems, dc distribution systems for home appliances, power conditioning systems for fuel cells and photovoltaic, modeling and simulation, and power electronics. Dr. Lee is a recipient of the Outstanding Scientists of the 21st Century from IBC and listed on 2008 Ed. of Who's Who in America. He is an Associate Editor of the IEEE TRANSACTIONS ON INDUSTRIAL ELECTRONICS and the IEEE TRANSACTIONS ON POWERELECTRONICS. He was the General Chair for the IEEE Vehicular Power and Propulsion Conference, in 2012.

Chung-Yuen Won was born in Korea, in 1955. He received the B.S degree in electrical engineering from the Sungkyunkwan Univ. Korea, in1978. And he received the M.S and Ph. D degree in electrical engineering from the Seoul National University, Korea, in 1980 and 1987, respectively. During 1990~1991 he had been in visiting professor, Department of electrical engineering, University of Tennessee. Since 1988 he has been with the faculty of Sungkyunkwan University, where he is a professor of School of Information and Communication Engineering. His research interests include dc-dc converter for Fuel Cell, electromagnetic modeling and prediction for motor drive, control systems for rail power delivery applications areas of stability of ac machines, advanced control of electrical machines, and power electronics.